RESEARCH ARTICLE

Synthesis and Characterization of Ce Doped MgO Nanocrystals

R. Poonguzhali[1]*, R. Gobi[2], M. Shanmugam[1], V. Karthik[1]

[1]Department of Physics, Mahendra Arts and Science College, (Autonomous), Kallipatti, 637501, Tamilnadu, India.
[2]Department of Physics, Arignar Anna Government Arts College, Namakkal, 637002, Tamilnadu, India.

ABSTRACT: Ce-doped MgO nanopowders were prepared via a chemical coprecipitation method. The as-obtained products were characterized by X-ray diffraction (XRD), scanning electron microscope (SEM), Thermo gravimetric and differential thermal analysis (TG-DTA) and UV diffused reflectance spectroscopy (UV DRS). The results show that cerium atoms have been successfully incorporated into the crystal lattice of MgO with cubic structure. SEM with EDX and XRD characterization studies confirmed that MgO particles thus obtained have hierarchical structures with high purity. The particles are uniformly spherical in shape. The elements presented in the sample were found by EDX. FTIR analysis confirmed the presence of Mg-O stretching in the sample. The perspective applications of the synthesized materials include photocatalysis (e.g. reduction of CO_2, degradation of CH_3 CHO, dye degradation, etc), dye sensitized solar cells, nanofluids with high thermal conductivity and heavy metal ions removal.

KEYWORDS: Nanocrystals, undoped and Ce doped MgO, Supercapacitor.

1. INTRODUCTION

The study of metal oxides has attracted the attention of material scientists due to their optical, electrical, magnetic, mechanical and catalytic properties which make them technologically useful. Nanostructures of metal oxides have been recently become the subject of extensive research due to their potential applications such as functional components for nanoelectronics, optoelectronics and sensing devices [1]. The relation between the structure and properties (both physical and chemical) of oxide materials and their applications are of great importance. Metal oxides such as MgO, ZnO, CdO, Ga_2O_3, In_2O_3, TiO_2, and SnO_2 have been explored in this regard [2-3].

Currently considerable interest in Nanocrystalline oxide materials exists owing to their unusual properties. Decreasing particle size results in some remarkable phenomenon. It has been found that smaller the particles, the higher the catalytic activity (Pt/ Al_2O_3), higher the mechanical reinforcement (carbon black in rubber), higher the electrical conductivity in ceramics (CeO_2), Higher the photo catalytic activity. Superparamagnetic behavior of magnetic oxides and higher the Blue shift of optical spectra of quantum dots.

Unusual optical and electrical properties in these materials take place due to a phenomenon known as Quantum Confinement. Nanocrystals of common metal oxides such as MgO, CaO, ZnO, TiO_2, and Al_2O_3 have been shown to be highly efficient and active absorbants for many toxic chemicals including air pollutants, chemical warfare agents, and acidic gases. Metal oxides like Fe_2O_3, $BaFe_{12}O_{19}$ are used as cancer detection and remediation, sensors and memory devices due to its Superparamagnetic behaviour [4].

Among these Magnesium Oxide (MgO) has many potential applications in almost all the areas both industrial and commercial purposes. MgO has applications in catalysis, toxic waste remediation, as additives in refractory, paint and superconductor products and in steel manufacturing because of its high corrosion-resistant behaviour [5]. With its excellent thermo dynamical stability, low Dielectric constant and low Refractive index it has been used as a transition layer for growing various thin films. It is widely used for cleaning fuel oil pipelines, avoiding sludge formation in tanks, protection of boilers against corrosion, thereby increasing these systems lifetimes [6-7]. MgO is used as an insulator in industrial cables and devices that exhibit the tunnel magneto resistant effect. It is also used as a basic refractory material for lining crucibles. Due to its excellent diffusing and reflectivity properties, it is used as a reference white color in calorimetry.

MgO is used as a medication to relieve heartburn, sour stomach and acid indigestion. It is a principle ingredient in construction materials and hence used for fire proofing [8]. It is used as one of the raw materials for making cement in dry process plants. Due to its high dielectric strength and average thermal conductivity, it is extensively used in electrical heating elements. MgO has also applications in pharmaceuticals, semiconductors liquid crystal /electroluminescent / plasma / fluorescent displays, reflecting and anti reflecting coatings where its electro-optical properties are used to advantage [9]. It has also wide applications in the insulating and buffer layers of multilayer electronic/ photonic devices owing to its very large band gap, excellent thermal stability and electrical insulating properties. Magnesium based alloys are found advantageous for various devices in the field of electronics, aerospace, automotive applications and biomedicine [10].

Though MgO has many potential applications, the control of basic properties is still a challenge. By tuning the particle size and controlling the morphology of the MgO nanoparticles, we can get efficient applications.

***Corresponding Author:** kuzhaliphy@gmail.com

Received: 19.03.2017 **Accepted:** 14.04.2017 **Published on**: 27.05.2017

We found that the Mg particle size and morphology were easily controlled by changing the Ce dopant ratio and MgO particles as small as 28 nm were obtained without stabilizer addition. Their hydrogen storage properties including thermodynamics and kinetics are discussed in the context of particle size evolution.

2. Materials and Methods

2.1. *Chemicals*

Magnesium nitrate hexahydrate [$Mg(NO_3)_2.6H_2O$], the precursor for Magnesium, potassium hydroxide (KOH), the oxide source, Cerium nitrate hexahydrate [$Ce(NO_3)_3.6H_2O$], the doping agent, were purchased from Merck. All chemicals were used as received since they were of analytical regent grade with 99 % purity..

2.2. *Synthesis of undoped and Ce doped MgO nanocrystals*

For the synthesis of Ce-doped MgO, 0.5 M of magnesium nitrate dissolved in 50 ml of deionized water was stirred vigorously by magnetic stirrer and cerium nitrate with different mole percentages (0.05, 0.075 and 0.1 M) prepared in 20 ml aqueous were mixed drop by drop. Then, 2 M of potassium hydroxide in 50 ml of deionized water was added drop by drop to the above mixture. The entire mixture was stirred magnetically 4 hrs at room temperature until a white precipitate was formed. The obtained dispersions were purified by dialysis against de-ionized water and ethanol several times to remove impurities. The yield products were dried in hot air oven at 100 °C for 6 h to evaporate water and organic materials to the maximum extent. To obtain the pure phase of MgO the precursor was annealed at 450°C for 2 hrs. The dried powders were pulverized to fine powders using agate mortar for further characterizations. A similar method of preparation without the addition of cerium was used to synthesize undoped MgO nanocrystals.

3. RESULTS AND DISCUSSION

3.1. *Thermo Gravimetric-Differential Thermal analysis (TG-DTA)*

The thermal behavior of as prepared precursor MgO is recorded in the range of room temperature to 600°C in the presence of nitrogen atmosphere. Fig.**1** shows the TGA/DTA curves of the as-prepared magnesium hydroxide. The TGA curve shows three weight losses. The first small weight loss observed below 132 °C (5 %) is related to the loss of free water and the second weight loss between 132-301 °C (7.5 %) is attributed to decomposition of organic templates. The major weight loss in the temperature range of 289 °C - 450 °C is related to decomposition of $Mg(OH)_2$ and crystallization of MgO nanoparticles. The strong endothermic peak observed at about 350 °C in the DTA curve could be attributed to the decomposition of Mg $(OH)_2$, into MgO as given by the equation.

$$Mg(OH)_2 \leftrightarrow MgO + H_2O \text{ --------[1]}$$

The observed weight loss predicted from 301 °C to 455 °C is 31 wt %, which is in a good agreement with the theoretical value from Mg $(OH)_2$ to MgO transformation (30.8 wt.%) [11].

3.2 X-Ray Diffraction (XRD)

X-ray diffraction (XRD) patterns of undoped and various levels of (0.05, 0.075, and 0.1 M) Cerium doped MgO nanocrystals are displayed in Fig.3.2. All the diffraction patterns can be indexed as a face-centered cubic phase of periclase MgO (JCPDS No: (78-0430) with space group of Fm3m. The XRD peaks are assigned to (100), (111), (200) and (220) atomic planes indicating MgO phase [12-13]. In addition, narrow peaks with high intensities indicate good crystallinity of the as-prepared nanoparticles. The estimated unit cell constant is a = 4.265 Å for MgO particles confirms that the sample is formed in a single phase and the value of unit cell constant is slightly decreased on Ce doping which may be due to the introduction of cerium in MgO (a = 4.259 Å).

Considerably, broadened lines in the XRD patterns are indicative of the presence of nano-size particles. We have used the (200) reflection, like in the XRD patterns, for obtaining the average particle size with the help of Debye–Scherrer's eqn. [14].

$$D = 0.9\lambda/\beta\cos\theta \text{ ----------[2]}$$

Where β is full width at half maxima of the peak in XRD pattern, θ is diffraction angle, λ is X- ray wavelength, respectively. The structural parameters such as lattice constant, dislocation density and micro strain were calculated for the undoped and Ce - doped samples and listed in Table 3.1. As far as micro strain is concerned, smaller sized particles have high value of strain and larger particles show smaller strain value.

3.3 Functional group analysis

In order to analyze the functional groups present in the pure and Ce-doped MgO samples, the FT-IR spectra were recorded in the range of 400-4000 cm^{-1}.The FT-IR spectrum of undoped and various levels of (0.05, 0.075, and 0.1 M) Cerium doped MgO nanocrystals are shown in Fig. 3. The characteristic vibrational mode of symmetric MgO_6 octahedral of MgO was obtained at 418 cm^{-1}. The absorption at 3697 cm^{-1} indicates the presence of hydroxyl groups (surface adsorbed). After calcination at higher temperature, the absorption in the range of 1300–1800 cm^{-1} related to hydroxyl group of molecular water at 1641 cm^{-1} and to NH_3 at 1440 cm^{-1} [15-16]. Further, the peaks at 550–850 cm^{-1} (δ_1) indicate the higher frequency of MgO stretching and 410 – 450 cm^{-1} (δ_2) is lower frequency stretching [17-18].

3.4 UV-Vis Absorption Spectra

Fig. 4 shows the optical absorption spectra of MgO and Ce doped with different levels (0.025, 0.05 and 0.075M) of MgO ions. The absorption edges of the as prepared undoped and different levels of Ce doped MgO are 221.12, 222.02, 220.4 and 223.61 nm, respectively. The optical bandgap of MgO particles was found using the formula [19-20].

$$E_g\,(eV) = 1240 / \lambda \text{ ----------[3]}$$

in which 'λ_g' is the wavelength of the intercept. The band gaps were found to be 5.62 eV (MgO), 5.60 eV (0.05 M Ce), 5.64 eV (0.075 M Ce) and 5.56 eV (0.1 M Ce), respectively. MgO is a wide band gap insulator having band gap 7.8 eV in its bulk form [21]. A large difference in the optical band gap of the nanoparticles obtained as compared to their bulk particles.

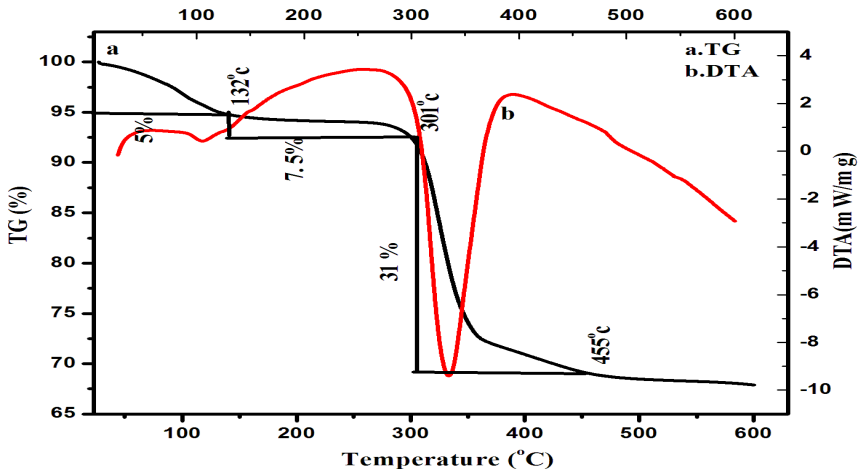

Fig.1: TG-DTA curves of precursors of MgO nanocrystals

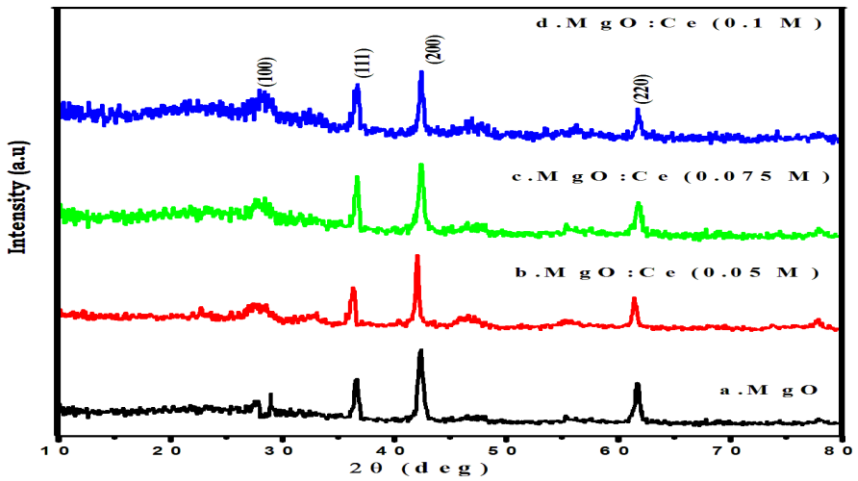

Fig 2: XRD patterns of pure and various levels of (0.05, 0.075 and 0.1 M) Ce doped MgO nanocrystals

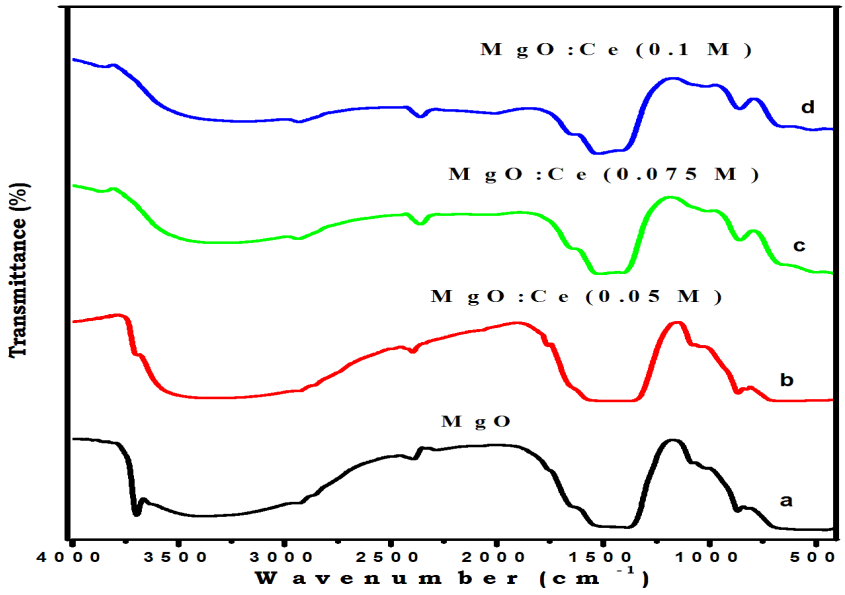

Fig. 3. FTIR Spectrum of as - prepared pure and Ce - doped MgO nanocrystals

Table 1. Crystallite size, Lattice parameters, and strain of MgO doped with different levels of cerium.

Samples	Average particle size from XRD peak (nm)	Lattice constant (Á)		Micro strain ε x $10^{-3}lin^{-2}m^{-4}$
		Calculated value	Standard value	
Pure (MgO)	17.399	a=4.265	a=4.212	8.017
0.05 M Ce doped MgO	24.789	a=4.259	a=4.212	7.040
.075 M Ce doped MgO	28.888	a=4.258	a=4.212	6.879
0.1 M Ce doped MgO	28.907	a=4.257	a=4.212	6.870

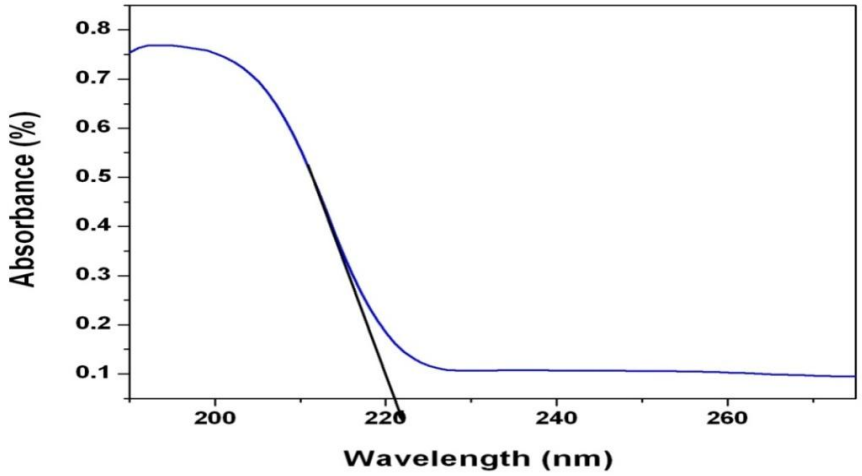

Fig. 4(a): Optical Absorption spectrum of MgO nanoparticles

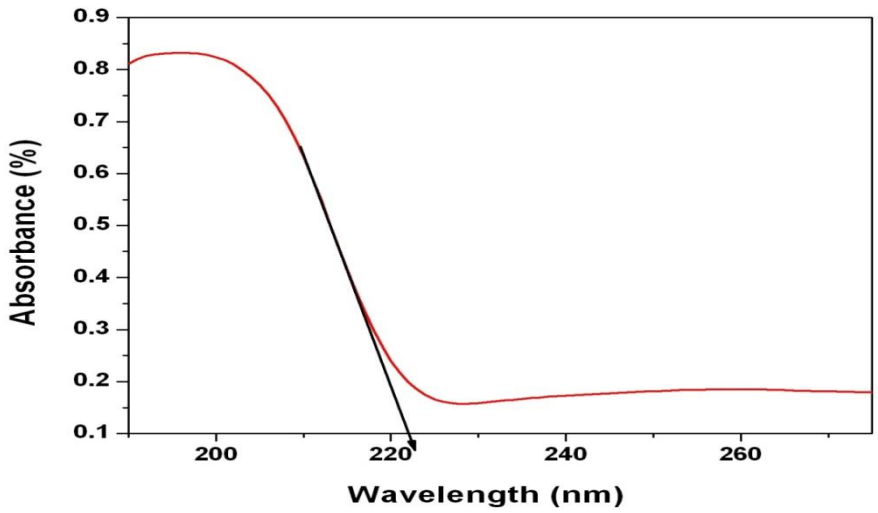

Fig. 4(b): Optical Absorption spectrum of 0.05 M of Ce doped MgO nanoparticles

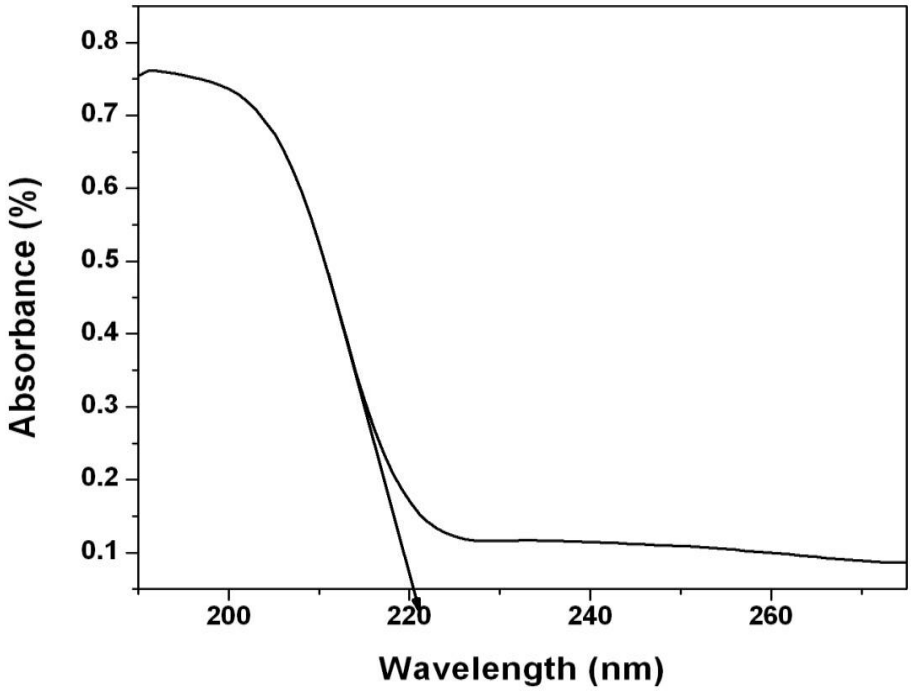

Fig. 4(c): Optical Absorption spectrum of 0.075 M of Ce doped MgO nanoparticles

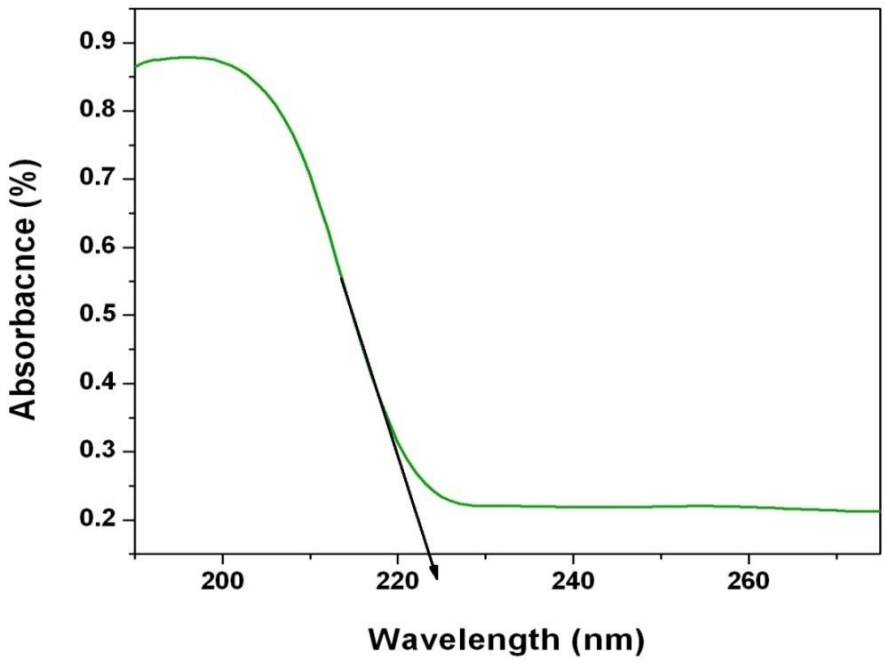

Fig. 4(d): Optical Absorption spectrum of 0.1 M of Ce doped MgO nanoparticles

3.5. *Morphological Observations*

Figure 5a shows the non-homogeneous distribution of MgO particles with spherical morphology. The sizes of the particles are in the range of 30-40 nm. Fig. 5b reveals the agglomerated spherical as well as plate like morphology of MgO on 0.1 M of Ce - doping. From the figure, it is seen that the particles are having spherical morphology. EDX spectrum indicates the presence of Mg and O [22, 23]. The EDX spectrum of 0.1 M of Ce - doped MgO reveals the presence of Mg, O and Ce. It is also evident to notice that the prepared Ce - doped MgO compositions are pure and free of elemental impurities (Fig. 5c).

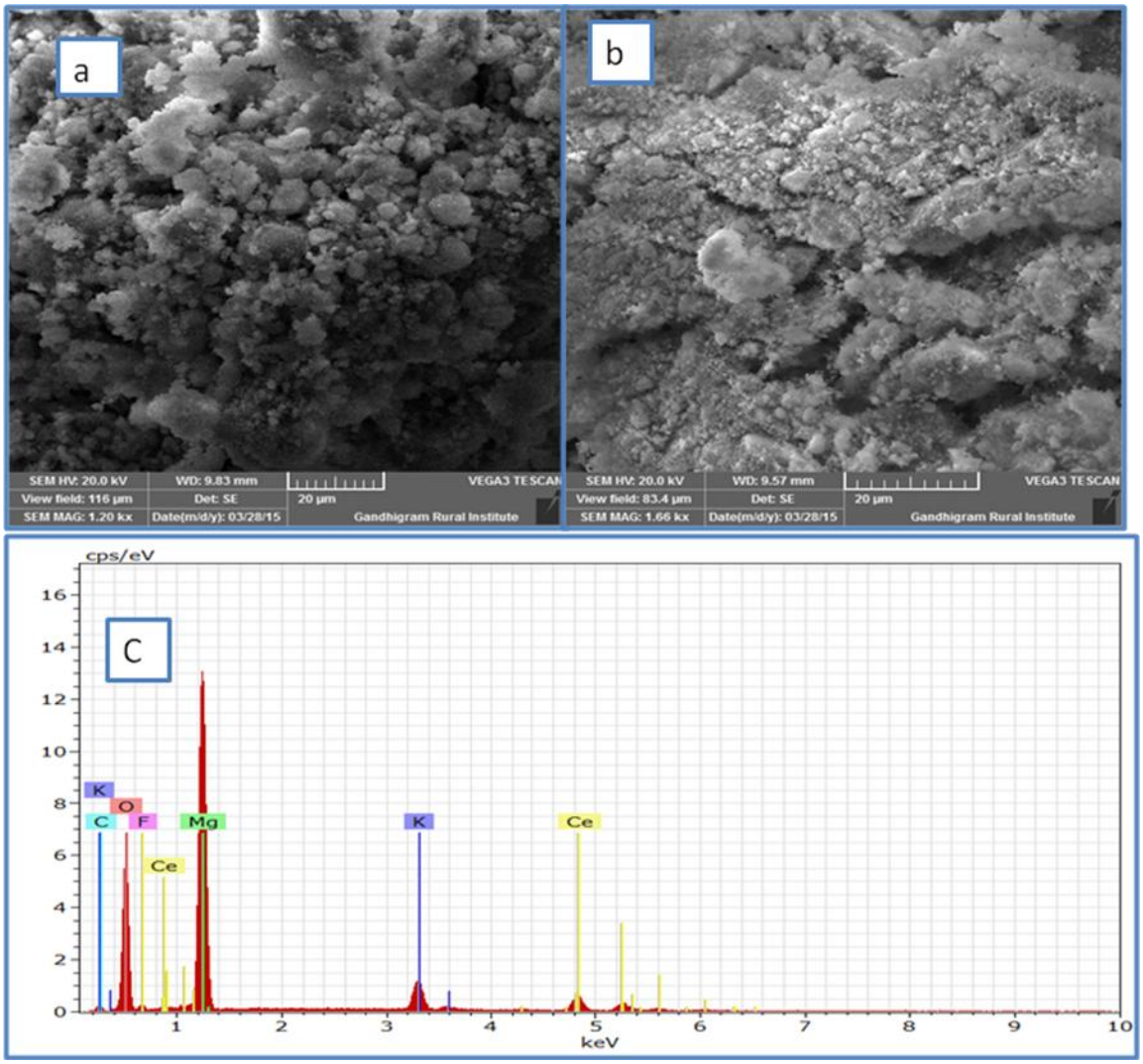

Fig. 5: SEM images of (a) pure and Ce - doped (0.1 M) MgO (b) and EDX spectrum of 0.1 M of Ce - doped MgO nanoparticles (c).

4. CONCLUSION

The present study demonstrates the effect of Ce on the structural, morphological, and optical properties of MgO nanostructures through a simple chemical precipitation method. The samples were analyzed for thermal studies. Thermal analysis results revealed that 450°C could be the optimum level of annealing for the harvest of pure phase of MgO. Further, the products annealed at 450°C were analyzed for their structural, optical, morphological and magnetic properties. The XRD patterns revealed that the particles exhibit a pure cubic structure. The estimated sizes of the nanoparticles were in the range of 17-28 nm. The FT-IR spectra confirmed the formation of the MgO nanostructures. The Optical properties of MgO and Ce doped MgO nanoparticles showed a large difference in optical band gap as compared to their bulk counterpart. SEM analysis shows the formation of spherical shape morphology with sizes ranging between 30 and 40 nm. The perspective applications of the synthesized materials include photocatalysis (e.g. reduction of CO_2, degradation of CH_3 CHO, dye degradation, etc), dye sensitized solar cells, nanofluids with high thermal conductivity and heavy metal ions removal.

REFERENCES

[1]. Wang,B, Hang,H, Xian,T, Di,L.J, Li,R.S, Wang,X.X, 2015. Synthesis of spherical $Bi2WO_6$ nanoparticles by a hydrothermal route and their photocatalytic properties, J. of Nanomaterials,16,(1),194.

[2]. Yuanjie Mao, Minghao Fang, Zhaohui Huang Haitao Liu, Shuyue Liu, Yan-gai Liu, Xiaowen Wu, Xin Min, Chao Tang, Hao Tang and Hui Wu, 2015. Fabrication of morphology-controlled MgO nanowhiskers and nanocrosses by magnesiothermic synthesis in vapor phase at 550 °C , *RSC Adv.*, 5, 62747-62751

[3]. Hyoun Woo Kim, Seung Hyun Shim, and Ju Hyun Myung, 2005. Synthesis and Characteristics of SnO_2 Nanorods on Pd-Coated Substrates, *Brazilian Journal of Physics, 35, 4A.*

[4]. Kalyanikutty K.P., F.L. Deepak, C. Edem, A. Govindaraj, Rao,CNR, 2005. Carbon-assisted synthesis of nanowires and related nanostructures of MgO, Materials Research Bulletin, 40, 831-839.

[5]. Foster L.E., 2006. Nanotechnology, Personal Education, New Delhi, 143-145.

[6]. Kumari L., W.Z. Li, C.H. Vannoy, R.M. Leblanc, D.Z. Wang, 2009. Synthesis, characterization and optical properties of Mg $(OH)_2$ micro-/nanostructure and its conversion to MgO, Ceramic International, 35, 3355-3364.

[7]. Shah M.A., A. Qurashi, 2009. Novel surfactant-free synthesis of MgO nanoflakes, Journal of Alloys and Compounds, 482, 548-551.

[8]. Duan G., X. Yang, J. Chen, G. Haung, L. Lu, X. Wang, 2007. The catalytic effect of nanosized MgO on the decomposition of ammonium perchlorate", Powder Technology, 172, 27-29.

[9]. A. Tadjarodi, M. Sedghi, K. Bijanzad, 2012. Synthesis and Charaterization of Magensium Oxide Mesoporous Microstructures Using Pluronic F127, JNS 2, 273-278.

[10]. Kumar A., J. Kumar, 2008. On the synthesis and optical absorption studies of nano-size MgO powder. Journal of Physics and Chemistry of Solids, 69, 2764-2772.

[11]. Qiu T., X.L. Wu, F.Y. Jin, A.P. Huang, P.K. Chu, 2007. Self-assembled growth of MgO nanosheet arrays via a micro-arc oxidation technique, Applied Surface Science, 253, 3987-3990.

[12]. Fereshteh Meshkani, Mehran Rezaei, 2010. Effect of process parameters on the synthesis of nano crystalline magnesium oxide with high surface area and plate-like shape by surfactant assisted precipitation method, Powder Technology 199, 144–148.

[13]. Ramanujam K., M. Sundrarajan, 2014. Antibacterial effects of biosynthesized MgO nanoparticles using ethanolic fruit extract of Emblica officinalis, J. Photochem. Photobiol. B. 141, 296–300.

[14]. Venkatesha T.G., Y.A. Nayaka, B.K. Chethana, 2013. Adsorption of Ponceau S, from aqueous solution by MgO nanoparticles, Appl. Surf. Sci. 276, 620–627.

[15]. Park N.G., M.G. Kang, K.S. Ryu, K.M. Kim, S.H. Chang, 2004. Photovoltaic characteristics of dye-sensitized surface-modified nanocrystalline SnO_2 solar cells, J.Photochem. Photobiol. A: Chem. 161, 105.

[16]. Hassouna D., C. Hedia, T. Fathi, $Mg(OH)_2$ 2011. Nanorods synthesized by a facile hydrothermal method in the presence of CTAB, Nano-Micro Lett. 3, 153–159.

[17]. Wu X., H. Cao, G. Yin, J. Yin, Y. Lu, B. Li, 2011. $MgCO_3$ $3H_2O$ and MgO complex nanostructures: controllable biomimetic fabrication and physical chemical properties, Phys. Chem. Chem. Phys. 13, 5047–5052.

[18]. Selvamani T., T. Yagyu, S. Kawasaki, I. 2010. Mukhopadhyay, .Effects of Cationic Surfactant in Sol-gel Synthesis of Nano Sized Magnesium Oxide, Catal. Commun. 11, 537–541.

[19]. Borghei S. M., S. Kamali, M.H. Shakib, A. Bazrafshan, M.J. Ghoranneviss, 2010. Luminescence properties of MgO: Fe^{3+} nanopowders for WLEDs under NUV excitation prepared via propellant combustion route, J. Fusion Energy 30, 433–436.

[20]. Latha Kumari, W.Z. Li, Charles H. Vannoy, Roger M. Leblanc, D.Z. Wang, 2009. Synthesis, Characterization and Optical Properties of $Mg(OH)_2$ Micro-/Nanostructure and Its Conversion to MgO, Ceram. Int. 35, 3355–3364.

[21]. Ren L., Y.P. Zeng, D. Jiang, 2010. Xylene gas sensor based on Ni doped TiO_2 bowl-like submicron particles with enhanced sensing performance, Solid State Sci. 12, 138–143.

[22]. Zhang G.Q., N. Chang, D.Q. Han, A.Q. Zhou, X.H. Xu, 2010. Sol-Gel-Hydrothermal Synthesis of the Heterostructured - Composite with High-Visible-Light- and Ultraviolet-Light-Induced Photocatalytic Performances, Mater. Lett. 64, 2135–2137.

[23]. Tamboli S.H., R.B. Patil, S.V. Kamat, V. Puri, R.K. Puri, 2009. Modification of optical properties of MgO thin films by vapour chopping, Journal of Alloys and Compounds, 477, 855-859.